

AFOLABI, R.O., YUSUF, E.O., OKONJI, C.V. and NWOBODO, S.C. 2019. Predictive analytics for the Vipulanandan rheological model and its correlative effect for nanoparticle modification of drilling mud. Journal of petroleum science and engineering [online], 183, article ID 106377. Available from:
<https://doi.org/10.1016/j.petrol.2019.106377>

Predictive analytics for the Vipulanandan rheological model and its correlative effect for nanoparticle modification of drilling mud.

AFOLABI, R.O., YUSUF, E.O., OKONJI, C.V., NWOBODO, S.C.

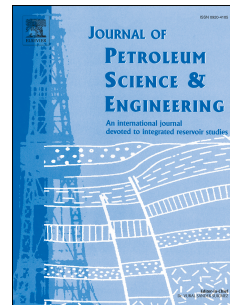
2019



Journal Pre-proof

Predictive analytics for the Vipulanandan rheological model and its correlative effect for nanoparticle modification of drilling mud

Richard O. Afolabi, Esther O. Yusuf, Chude V. Okonji, Shalom C. Nwobodo



PII: S0920-4105(19)30798-3

DOI: <https://doi.org/10.1016/j.petrol.2019.106377>

Reference: PETROL 106377

To appear in: *Journal of Petroleum Science and Engineering*

Received Date: 16 March 2019

Revised Date: 12 July 2019

Accepted Date: 12 August 2019

Please cite this article as: Afolabi, R.O., Yusuf, E.O., Okonji, C.V., Nwobodo, S.C., Predictive analytics for the Vipulanandan rheological model and its correlative effect for nanoparticle modification of drilling mud, *Journal of Petroleum Science and Engineering* (2019), doi: <https://doi.org/10.1016/j.petrol.2019.106377>.

This is a PDF file of an article that has undergone enhancements after acceptance, such as the addition of a cover page and metadata, and formatting for readability, but it is not yet the definitive version of record. This version will undergo additional copyediting, typesetting and review before it is published in its final form, but we are providing this version to give early visibility of the article. Please note that, during the production process, errors may be discovered which could affect the content, and all legal disclaimers that apply to the journal pertain.

© 2019 Published by Elsevier B.V.

1 **Research Article**

2 **Title:** Predictive Analytics for the Vipulanandan Rheological Model and its Correlative
3 Effect for Nanoparticle Modification of Drilling Mud.

4 **Authors:** Richard O. Afolabi ^{1, 3, *}, Esther O. Yusuf ², Chude V. Okonji³, Shalom C.
5 Nwobodo³

6 **Affiliations:** ¹ School of Engineering, Robert Gordon University, Aberdeen, AB10 7GJ,
7 United Kingdom

8 ² Department of Chemical Engineering, Covenant University, P.M.B 1023, Ota, Ogun State,
9 Nigeria.

10 ³ Department of Petroleum Engineering, Covenant University, P.M.B 1023, Ota, Ogun State,
11 Nigeria.

12 ***Contact email:** r.afolabi@rgu.ac.uk; richard.afolabi@covenantuniversity.edu.ng

13

14

15

16

17

18

19

20

Abstract

Modelling the flow of nanoparticle modified drilling mud (or nano-drilling muds) requires the use of existing generic time-independent models with the addition of nanoparticle terms having a number of parameters incorporated. These parameters quantify the uncertainties surrounding nanoparticle contributions to drilling mud rheology. However, when the parameters in the overall model become too large, the tuning of each parameter for proper flow description can be challenging and time-consuming. In addition, the predictive capability of known models for the different regimes associated with the flow of nano-drilling muds is limited in scope and application. For example, computational analysis involving nano-drilling muds have been described using Herschel-Buckley, Power-Law, Bingham Plastic, Robertson-Stiff, Casson, Sisko, and Prandtl-Eyring. However, these models have been shown over time to have limited predictive capability in accurately describing the flow behavior over the full spectrum of shear rates. Recently, a new rheological model, the Vipulanandan model, has gained attraction due to its extensive predictive capability compared to known generic time-independent models. In this work, a rheological and computational analysis of the Vipulanandan model was carried out with specific emphasis on its modification to account for the effects of nanoparticles on drilling muds. The outcome of this novel approach is that the Vipulanandan model can be modified to account for the effect of interaction between nanoparticles and clay particles. The modified Vipulanandan show better prediction for a 6.3 wt.% mud with R^2 of 0.999 compared to 0.962 for Power law and 0.991 for Bingham. However, the R^2 value was the same with Herschel Buckley model but the RMSE value show better prediction for the Vipulanandan model with a value of 0.377 Pa compared to the 0.433 Pa for Herschel Buckley model.

Keywords: Drilling Mud; Bentonite Mud; Vipulanandan; Nanoparticles; Rheology, Modelling

46

47 **1. Introduction**

48 The description of the rheology of drilling muds is essential for an adequate determination of
 49 hydraulic conditions such as velocity profile and pressure loss emanating during drilling
 50 activities (Toorman, 1997). This is also significant in the estimation of the hole cleaning
 51 efficiency of the drilling mud (Toorman, 1997; Abdo and Danish Haneef, 2012; Hoelscher et
 52 al., 2012; Jung et al., 2013; Ismail et al., 2016; Afolabi et al., 2017a). Therefore,
 53 computational modelling of the velocity profile, pressure loss and hole cleaning efficiency
 54 during drilling requires models which can approximate the rheology of the mud. The
 55 application of known rheological models in the description of the flow behavior of drilling
 56 muds necessitates that its predictive capability correlates with certain conditions.
 57 Mathematically, Vipulanandan and Mohammed (2014) described these conditions as shown
 58 in equations (1) to (4):

$$59 \lim_{\dot{\gamma} \rightarrow 0} \tau = \tau_0 \quad (1)$$

$$60 \frac{d\tau}{d\dot{\gamma}} > 0 \quad (2)$$

$$61 \frac{d^2\tau}{d\dot{\gamma}^2} < 0 \quad (3)$$

$$62 \lim_{\dot{\gamma} \rightarrow \infty} \tau = \tau_{\max}$$

$$63 \quad (4)$$

64 Where τ_0 is the yield point, τ is the shear stress and $\dot{\gamma}$ is the shear rate of the drilling mud.
 65 Equation (1) simply describes the yield point of the drilling mud. This is the minimum shear
 66 stress that must be exceeded for the drilling mud to flow. Furthermore, it is a measure of the
 67 pumping ability of the drilling mud and its efficiency in the removal of drilled cuttings under
 68 static and dynamic conditions respectively (Kelessidis and Maglione, 2008; Abu-Jdayil,

69 2011; Lee et al., 2012; Yoon and El-Mohtar, 2013; Vipulanandan and Mohammed, 2014;
70 Afolabi et al., 2017a; Afolabi and Yusuf, 2018). In addition, equation (2) indicates that the
71 drilling mud must possess sufficient viscosity in order to keep the weighting materials and
72 drilled cuttings suspended during continuous mud circulation. The absence of sufficient
73 viscosity would result in the cuttings or weighting materials settling out of suspension when
74 mud circulation is stopped (Fazelabdolabadi et al., 2015; Ismail et al., 2016; Afolabi et al.,
75 2017a; Afolabi et al., 2017b; Afolabi and Yusuf, 2018). The thixotropic nature of drilling
76 muds is captured in equation (3) where there is a reversible decrease in viscosity with shear
77 rate and increase in viscosity when the shear is removed. Moreover, the maximum shear
78 stress tolerance of the drilling mud is captured in equation (4). The shear stress limit of a
79 drilling mud indicates its erosive capability which is an important function of drilling muds
80 (Vipulanandan and Mohammed, 2014; Afolabi et al., 2017b; Afolabi and Yusuf, 2018).
81 Besides the breaking of rocks by the drill bit, the drilling muds must also contribute to this
82 through its erosive potential. Accordingly, the need for an efficient drilling mud system made
83 from bentonite suspensions has resulted in research into nanotechnology (Zakaria et al., 2012;
84 Mahmoud et al., 2016; Afolabi et al., 2017b; Afolabi and Yusuf, 2018). However,
85 computational modelling of nanoparticle effect on the flow behavior of drilling mud is still
86 limited in scope and application with reliance placed on existing models such as Herschel-
87 Buckley, Power-Law, Bingham Plastic, Robertson-Stiff, Casson, Sisko, and Prandtl-Eyring.
88 In addition, generic rheological models used in the petroleum industry would give a
89 generalized approach to computing the performance of nano-drilling muds without
90 adequately capturing contributions due to nanoparticles (Reilly et al., 2016; Afolabi et al.,
91 2017a; Afolabi et al., 2017b; Afolabi and Yusuf, 2018; Gerogiorgis et al., 2017; Vryzas and
92 Kelessidis, 2017). Consequently, the use of existing time independent rheological models in
93 its present form for nano-drilling muds would require a data-driven approach where models

94 are regressed to shear stress-shear rate values. Nevertheless, Reilly et al. (2016) and
 95 Gerogiorgis et al. (2017) derived a multivariate rheological model from first principles which
 96 describe the flow behavior of nanoparticle modified drilling muds. The shear stress of the
 97 nano-drilling mud was dependent on the volume fraction of nanoparticles, size of
 98 nanoparticles and shear rate with good correlation at high shear rates. The multivariate model
 99 developed by the authors followed the expression in equation (5):

$$100 \quad \tau = \tau_y + \tau_\infty + \tau_{np} \quad (5)$$

101 where τ_y is the yield stress of the mud, τ_{np} is the shear stress of the mud due to nanoparticles
 102 and τ_∞ is the shear stress ascribed to the constant viscosity of a drilling mud measured at
 103 high shear rates. Equation (6) shows the model derived by the authors by applying the
 104 expression in (5):

$$105 \quad \tau = \tau_y + \mu_\infty \dot{\gamma} + \frac{A_o r_p}{12 A_p \left[4 r_p \left(\frac{1}{1 + \beta \dot{\gamma}} \right) + \left(1 - \frac{1}{1 + \beta \dot{\gamma}} \right) d_p^3 \sqrt{\frac{\pi}{6 \phi}} \right]^2} \quad (6)$$

106 Where A_o is the Hamaker constant, A_p is the area of nanoparticles, r_p is the radius of
 107 nanoparticles, d_p is the diameter of the nanoparticles, ϕ is the volume fraction of
 108 nanoparticles and β is a time constant. This modelling approach for nano-drilling mud is
 109 simply the addition of the Bingham plastic model with a term for nanoparticle. Equally, the
 110 modelling approach means that it is limited to a specific model (Bingham plastic model) and
 111 may not accurately describe the flow behaviour over the full spectrum of shear rates as
 112 indicated by (1) to (4). Nonetheless, the multi-parameter nature of the model generally would
 113 give a full description of the contribution of nanoparticles to drilling mud rheology. Table 1
 114 show some specific rheological models and their predictive capability based on the conditions
 115 represented in equations (1) to (4). Based on these conditions, the Vipulanandan model
 116 proposed by Vipulanandan and Mohammed (2014) has a good predictive capability in

117 accurately describing the flow behaviour over the full spectrum of shear rates. In this work,
 118 the Vipulanandan model was modified to account for the effect of nanoparticles. The
 119 development of the shear term for nanoparticles followed the procedure given by Reilly et al.
 120 (2016) and Gerogiorgis et al. (2017). However, the term for nanoparticles was modified in
 121 order to reduce the complexity of the resultant model for the purpose of regression analysis.
 122 The outcome of this novel approach is that the Vipulanandan model can be modified to
 123 account for the effect of interaction between nanoparticles and clay particles. This was
 124 achieved by considering the Hamaker constant in the modified Vipulanandan model as a
 125 tuning parameter. In addition, other effects such as temperature and salinity were captured
 126 without necessarily introducing new fitting parameter.

127 **2. Modification of the Vipulanandan Model**

128 *2.1 Dimensionless Structuring Term*

129 According to Toorman (1997), a dimensionless structuring parameter, λ can be used to
 130 describe the changing structure of cohesive sediment suspension such as drilling muds under
 131 varying shear rates, $\dot{\gamma}$. This expression is given below in (7) and it is obtained under a
 132 pseudo-equilibrium state.

$$133 \quad \lambda = \frac{1}{1 + \beta_i \dot{\gamma}} \quad (7)$$

134 Where β_i is a time constant which is a ratio of the thickening and thinning parameters of the
 135 fluid suspension.

136 *2.2 Vipulanandan Model and Dimensionless Structuring Term*

137 The Vipulanandan model proposed by Vipulanandan and Mohammed (2014) which has a
 138 limit on the shear stress for a drilling mud was considered among others for this study as
 139 shown in equation (8) below

$$140 \quad \tau = \tau_0 + \frac{\dot{\gamma}}{A+D\dot{\gamma}} \quad (8)$$

141 Where $\dot{\gamma}$ is the shear rate (s^{-1}), τ_0 is the yield stress (Pa), A ($[Pas]^{-1}$) and D (Pa^{-1}) are
 142 model parameters or constants respectively. The shear erosive potential of the drilling mud
 143 can be predicted by its shear stress limit, τ_{lim} according to equation (9).

$$144 \quad \lim_{\dot{\gamma} \rightarrow \infty} \tau = \tau_{lim} = \tau_0 + \frac{1}{D} \quad (9)$$

145 The ratio of the model constants (D/A) represents a time constant denoted β_1 and this can be
 146 represented as shown in (10)

$$147 \quad \beta_1 = \frac{D}{A} \quad (10)$$

148 Modifying equation (8) to take into account this time constant yields equation (11) with
 149 $\beta_2 = 1/A$ (Pas).

$$150 \quad \tau = \tau_0 + \frac{\beta_2 \dot{\gamma}}{1+\beta_1 \dot{\gamma}} \quad (11)$$

151 Comparing (11) with (7) yields

$$152 \quad \tau = \tau_0 + \lambda \beta_2 \dot{\gamma} \quad (12)$$

153 This indicates that the Vipulanandan model has dimensionless structuring term which
 154 explains how the drilling mud structure changes monotonically from its initial state under
 155 zero shear rate to a final state under an infinite shear rate.

156 *2.3 Nanoparticle Modified Vipulanandan Model*

157 According to Reilly et al. (2016) and Gerogiorgis et al. (2017), the maximum interparticle
 158 distance between nanoparticles, H can be expressed as a function of the size of the
 159 nanoparticle, d_p and volume fraction of nanoparticles, ϕ

$$160 \quad H = d_p \sqrt[3]{\frac{\pi}{6\phi}} \quad (13)$$

161 However, in this work, H is considered the interparticle distance between nanoparticles in the
 162 presence and absence of shear. This can be related to the van der Waals force of attraction
 163 between nanoparticles as shown below (14).

$$164 \quad F_{vdw} = \frac{A_0 r_p}{12[H]^2} \quad (14)$$

165 A_0 is the Hamaker constant which provides the means to determine the interaction between
 166 particles. In order to understand how the van der Waals force of attraction between
 167 nanoparticles change under shear rates, the dimensionless structuring term is incorporated as
 168 follows

$$169 \quad F_{vdw} = \frac{A_0 r_p}{12[H]^2} \left(\frac{1}{1+\beta_3 \dot{\gamma}} \right) \equiv \frac{A_0 r_p}{12[H]^2 (1+\beta_3 \dot{\gamma})} \quad (15)$$

170 Substituting for H,

$$171 \quad F_{vdw} = \frac{A_0}{48 r_p \left[\frac{\pi}{6\phi} \right]^{2/3} (1+\beta_3 \dot{\gamma})} \quad (16)$$

172 Therefore, the shear stress due to nanoparticles, τ_{np} can be expressed as the van der Waals
 173 force per unit nanoparticle area, A_p .

$$174 \quad \tau_{np} = \frac{A_0}{48 A_p r_p \left[\frac{\pi}{6\phi} \right]^{2/3} (1+\beta_3 \dot{\gamma})} \quad (17)$$

175 Therefore, the modified form of the Vipulanandan model incorporating the effect of
 176 nanoparticles is given in (18)

$$177 \quad \tau = \tau_0 + \frac{\beta_2 \dot{\gamma}}{1+\beta_1 \dot{\gamma}} + \frac{A_0}{48 A_p r_p \left[\frac{\pi}{6\phi} \right]^{2/3} (1+\beta_3 \dot{\gamma})} \quad (18)$$

178 In order to account for the interaction between nanoparticles and bentonite clay, equation (18)
 179 is modified to have a tuning parameter, β_o

$$180 \quad \tau = \tau_0 + \frac{\beta_2 \dot{\gamma}}{1 + \beta_1 \dot{\gamma}} + \frac{\beta_o}{(1 + \beta_3 \dot{\gamma})} \quad (19)$$

181 Where $\beta_o = \left(A_o / \left[48 A_p r_p \left[\frac{\pi}{6\phi} \right]^{2/3} \right] \right)$ with units of Pa. This tuning parameter accounts for the
 182 uncertainty relating to the dispersion of nanoparticles and the assumption of spherical size for
 183 the nanoparticles. In addition, the value of β_o will change due to variation in the surface
 184 properties of the nanoparticles due to interaction with bentonite clay in drilling muds. This
 185 parameter would account for the contribution of these interactions to the shear stress profile
 186 of the drilling mud. The interaction between the nanoparticles and bentonite clay is assumed
 187 to be more of a physical interaction and as such, the prospects of a chemical reaction
 188 occurring is neglected. β_3 is considered a characteristic time constant associated with the
 189 interaction between clay and nanoparticles.

190 3. Material and Methods

191 3.1 Materials

192 The materials used in the study include commercial bentonite clay and silica nanoparticles
 193 (appearance: powder; colour: white; surface area: 60.2 m²/g, purity: 99.8 %, size: 50 ± 4 nm),
 194 which were purchased in Nigeria. Silica nanoparticles was considered due to its low toxicity
 195 and scalable availability arising from surface functionalization (Lieberman et al., 2014).

196 3.2 Formulation of Nanoparticle Modified Drilling Mud

197 The preparation of nanofluids was done in different concentrations containing 0.2, 0.4, and
 198 0.6 vol.% of silica nanoparticles dispersed in 400mL of deionized water respectively. A
 199 Hamilton beach mixer was used to continuously stir the nanoparticle dispersions until the
 200 formation of silica nanofluids. The nanofluids were the medium for dissolution of bentonite

201 clays thereby giving rise to nano-drilling muds. The stirring speed of the mixer was set to
202 11000-RPM. The nano-drilling mud was prepared by adding 6.3, 13 and 15 wt.% of bentonite
203 clay to different concentrations of nanofluids followed by mixing for 20 minutes. Subsequent
204 nano-drilling mud was prepared by increasing the bentonite content.

205 *3.3 Rheological Measurement*

206 The flow characteristics of the nano-drilling mud were evaluated using an OFITE Model 800
207 (8-Speed) Viscometer that is manufactured by OFI Testing Equipment, Inc. The rheological
208 behavior was obtained by measuring the shear stress at different shear rates. The shear rates
209 were simply altered with a speed regulator, which was done to sustain a continuous shear rate
210 under changing shear conditions and input power. The values for shear stress were shown on
211 an illuminated enlarged dial for easy reading. The dial readings (DR) from the viscometer
212 were taken at equilibrium values. The eight accurately controlled test speeds of the
213 viscometer (shear rates in RPM) are 3 (Gel), 6, 30, 60, 100, 200, 300, and 600.

214 **4. Results and Discussion**

215 *4.1. Comparison between Vipulanandan and other Rheological Models*

216 Comparison between the Vipulanandan model in equation (11) and the 2 most common
217 rheological models (Bingham and Herschel Buckley) employed in the oil and gas industry is
218 shown in Figure 1. For the Bingham Plastic model, the R^2 value of 0.991 and RMSE value
219 of 1.039 Pa was obtained for 6.3 wt.% bentonite mud. In the case of the Herschel Buckley
220 model, the base case mud of 6.3 wt.%, bentonite content was modelled with, R^2 value of
221 0.999 and RMSE value of 0.433 Pa respectively. The Vipulanandan model with shear stress
222 limit prediction was fitted with a R^2 value of 0.999 and RMSE value of 0.377 Pa for 6.3
223 wt.% bentonite mud. The Vipulanandan and Herschel Buckley models showed comparable
224 values for R^2 . However, the RMSE value for the Vipulanandan model was lower (0.377 Pa)

225 compared to the Herschel Buckley model (0.433 Pa). This indicates a better fitting of the
226 Vipulanandan model to the rheological data. Further comparison between the Vipulanandan
227 and Herschel Buckley models was done using the confidence and prediction intervals. Figure
228 2 show the 95 % confidence interval for the Vipulanandan and Herschel Buckley models.
229 The tapered confidence interval connected with the models is suggestive of their accuracy in
230 predicting the shear stress for a definite set of the predictor variable which is the shear rate.
231 Furthermore, in accessing the applicability of the Vipulanandan model, the uncertainty of
232 predicting the value of a single future observation or a fixed number of multiple future
233 observations based on the distribution of previous observations was evaluated. This was done
234 using the prediction interval, which is the range that is likely to contain a single future
235 response for a selected combination of variable settings. Figure 3 show the 95 % prediction
236 interval for the Vipulanandan and Herschel Buckley models. There is a 95 % probability that
237 future observation will be contained within the prediction interval. Therefore, the
238 Vipulanandan model shows comparable fitting attributes with the Herschel Buckley
239 rheological model employed in the oil and gas industry. However, the capability of the
240 Vipulanandan model is extended above the Herschel Buckley model due to its prediction of
241 the shear stress limit.

242 *4.2. The Effect of Bentonite Content at given Nanoparticle Concentration*

243 Figure 4 shows the fitted modified Vipulanandan model (equation 19) to a drilling mud
244 containing 13 and 15 wt.% bentonite clay and 0.2 vol.% silica nanoparticles. The model
245 shows good fitting to the rheological data irrespective of the bentonite clay content. The
246 model time constant, β_3 and tuning parameter, β_0 for the varied bentonite content is shown in
247 Table 2. The trend with bentonite content associated with the time constant and tuning
248 parameter are captured in Figure 5. The tuning parameter is assumed to account for the
249 dispersion and the level of interaction of particles arising from hydration in water. In

250 addition, the trend of the increase in the value of the tuning parameter show that the large
251 amount of clay particles may envelop the contribution of nanoparticles to the rheology of the
252 drilling mud. This is obvious from Figure 5(a) and it can be seen that beyond the bentonite
253 content of 13 wt.%, there is a rapid increase in the value of the tuning parameter. In this case,
254 the interaction between clay particles dominate the rheology of the nano-modified drilling
255 mud. This is apparent due to the large size of the clay particles compared to the silica
256 nanoparticles. The rise in the value of the time constant, β_1 (Table 2) explains the increased
257 interaction between clay particles dominating the rheology of the drilling mud. However, at
258 bentonite content less than 6.3 wt.%, the interaction between the silica nanoparticles and clay
259 particles may be considered to be more pronounced under these conditions. This phenomenon
260 may also explain the rapid rise in the characteristic time constant, β_3 up to bentonite content
261 of 6.3 wt.% (Figure 5(b)). The characteristic time scale for diffusion for the particles would
262 decrease due to an increase in the interaction between particles dominated by the larger clay
263 particles. Since the volume fraction of nanoparticles is kept constant, its interaction with clay
264 particles will diminish with an increasing amount of clay particles. This effect is evident
265 beyond the bentonite content of 6.3 wt.%, where there is a decline in the characteristic time
266 constant, β_3 (Figure 5(b)).

267 *4.3. The Effect of Nanoparticle Concentration at given Bentonite Content*

268 To study the effect of changing nanoparticle concentration at a given bentonite concentration,
269 Figure 6 shows a plot of the tuning parameter and the characteristic time constant for a 13
270 wt.% drilling mud containing 0.2 to 0.6 vol.% nanoparticles. The tuning parameter shows an
271 increasing trend with nanoparticle concentration as evident in Figure 6(a). This simply shows
272 the level of nanoparticle dispersion and the interaction associated with nanoparticles and clay
273 particles. In order words, the tuning parameter captures the contribution of this dispersion and
274 interaction to the overall shear stress profile of the drilling mud. This is consistent with the

275 units of the parameter (in Pa) which is similar to that of the shear stress. Additionally, the
276 values of the tuning parameter may indicate the nature of nanoparticle dispersion in the mud
277 solution. For low values of the tuning parameter reported in this work, this may indicate
278 aggregation of the nanoparticles in solution. As such, the dispersion of the nanoparticles in
279 the bentonite mud may not be nano-sized. However, there is need for more studies to be
280 carried out on the tuning parameter for different nanoparticle type and different dispersion
281 methods. The characteristic time constant, β_3 also showed an increasing trend with
282 nanoparticle concentration (Figure 6(b)). This indicates that increasing amount of
283 nanoparticles tend to interact with clay particles. Therefore, the characteristic timescale of
284 diffusion would increase because there is enough nanoparticles in solution to interact with
285 clay particles thereby altering the size and surface properties of both clay and nanoparticles.
286 For the time constant, β_1 , it can be observed from Table 3 that the values are low except at a
287 nanoparticle concentration of 0.6 vol.% and show no particular consistent trend. This stems
288 from the fact that clay to clay particle interaction are reduced due to an increase in the
289 amount of nanoparticles.

290 *4.4. Validating the Prediction of the Developed Model*

291 Statistical evaluation of the predictive capability of equation (19) was carried out using a
292 response surface design methodology (RSM). The RSM allowed for the generation of a
293 response surface model using the experimental data from the Nano-drilling mud. The
294 procedure was carried out using a central composite design to generate a design matrix (Table
295 4) for the study of single, interaction and quadratic effects between the factors bentonite
296 content (X_1) and nanoparticles, (X_2). MINITAB[®] 18 (PA, USA) statistical software package
297 was used for the design of experiments and statistical analysis. The response variable (Y) in
298 this case was the rheological properties (plastic viscosity PV, yield point YP, and apparent
299 viscosity AV) and was fitted to a second-order polynomial equation in (20):

$$300 \quad Y = \beta_{oi} + \sum_{i=1}^3 \beta_i X_i + \sum_{i=1}^3 \beta_{ii} X_i^2 + \sum_{i=0}^2 \sum_{j=i+1}^3 \beta_{ij} X_i X_j \quad (20)$$

301 Y : the predicted response; β_{oi} : the intercept coefficient; β_i : the linear coefficient; β_{ii} : the
 302 squared coefficient; β_{ij} : the interaction coefficient; X_i : the coded independent variables;
 303 $X_i X_j$: the interaction terms; X_i^2 : the quadratic terms. The statistical models obtained from
 304 regression analysis used in describing the response variable is given by the following second-
 305 order polynomial equation as shown in equation (21) to (23):

$$306 \quad PV = 0.0409 - 0.00918X - 0.0073Y + 0.000517X^2 + 0.0104Y^2 + 0.001884XY \quad (21)$$

$$307 \quad YP = 131.43 - 32.24X + 0.6Y + 1.8453X^2 - 8.2Y^2 + 1.003XY \quad (22)$$

$$308 \quad AV = 0.1693 - 0.04072X - 0.0047Y + 0.002324X^2 - 0.00204Y^2 + 0.002752XY \quad (23)$$

309 The obtained second-order response surface model above was used for the evaluation of the
 310 interaction effects on the rheological properties of the nano-drilling mud. However, before
 311 the analysis of interaction effects, there was a need to be certain that the developed surface
 312 model is capable of predicting the design matrix (Table 4). The coefficient of determination
 313 (R^2) for the obtained response surface models was 96.77, 99.73 and 99.81 % respectively for
 314 (21), (22) and (23) respectively. This indicates that the obtained statistical model is suitable
 315 for the design matrix since it is higher than 70 %. More so, it indicated that surface model can
 316 account for greater than 95 % variation in the design matrix while less than 5 % cannot be
 317 accounted for by the models from (21) to (23). Similarly, other statistical tools were used in
 318 addition to the coefficient of determination to determine the suitability of the response
 319 surface model. The probability value (P-value) for the fitted model was less than 0.05. This
 320 showed that the fitted model can confidently (> 95 %) investigate and predict the design
 321 matrix of equation (19). Other statistical evaluation tools such as confidence and prediction
 322 intervals are also considered. Figure 7 shows the 95 % confidence interval for equation (21).

323 The tapered confidence interval connected with the model is suggestive of the accuracy of the
 324 model in estimating the plastic viscosity for a definite set of the predictor variables (bentonite
 325 content and nanoparticles). Furthermore, in accessing the applicability of the proposed
 326 surface model, the uncertainty of predicting the value of a single future observation or a fixed
 327 number of multiple future observations based on the distribution of previous observations in
 328 the design matrix was evaluated. This was done using the prediction interval, which is the
 329 range that is likely to contain a single future response for a selected combination of variable
 330 settings. Figure 8 shows the 95 % prediction interval for the plastic viscosity using equation
 331 (21). From equations (21) to (23), the interaction between bentonite clay particles and
 332 nanoparticles tend to be captured by the interaction term XY. This term has a significant effect
 333 on the rheological properties due to its probability value less than 5 %. In addition, the
 334 positive coefficients of the interaction term suggest the incremental effect this has on the
 335 rheology of the drilling mud. This further validates the trends reported with tuning parameter,
 336 β_o and the characteristic time constant, β_3 of equation (19). The negative coefficients of the
 337 single terms X and Y suggests that individual particles cannot have an effect on the
 338 rheological properties.

339 4.5. Shear Stress Limit Prediction and Experimental Validation.

340 The shear erosive potential of the bentonite mud using equation (11) can be predicted
 341 according to equation (24).

$$342 \lim_{\gamma \rightarrow \infty} \tau = \tau_{lim} = \left[\tau_0 + \frac{\beta_2}{\beta_1} \right]$$

343 (24)

344 Where τ_{lim} (Pa) is the shear stress limit, which is a measure of the extent of shear stress
 345 tolerance of the bentonite mud. The shear stress limit was predicted using equation (20) for
 346 drilling mud containing 6, 9 and 11 wt.% bentonite dispersed. The values for the shear stress

347 limit predicted were 15.32, 33.71 and 63.8 Pa for 6, 9 and 11 wt.% bentonite respectively.
348 The experimental approach used in validating the predicted shear stress limit values was the
349 shear loading method. In this approach, a given shear rate (1022 s^{-1}), which corresponds to
350 the structural breakdown of the bentonite mud was applied using the OFITE model 800
351 viscometer for a period of 15 minutes. After a steady value for the dial reading (DR) was
352 obtained, the applied shear rate was reduced to zero and the gelling or recovery (structural
353 recovery) was noted for the same time period as the structural breakdown. The DR after the
354 recovery was then noted and the process was repeated until the DR after a structural
355 breakdown is constant. At this point, the bentonite mud has yielded and the DR was noted
356 and compared with the prediction as derived from equation (24). The values estimated from
357 the experiment compared to the predictions of the new model are summarized in Table 5. The
358 plots of the shear stress versus time showing the shear loading-shear recovery of the bentonite
359 mud is shown in Figure 9. The open markers refer to the point where the shear stress values
360 remain constant and approximate the predicted values for shear stress limit by equation (24).
361 Extending shearing time beyond what was applied in this study would result in a decrease in
362 the values of the DR beyond the shear stress limit. This is indicative of the structural
363 degradation of the bentonite mud and would result in an irreversible loss in viscosity.

364 **5. Conclusion and Recommendation**

365 This study was carried out to develop a new predictive approach to the modelling of the
366 rheological behavior of nano-drilling muds. The Vipulanandan model was selected based on
367 known conditions used in accessing the robustness and predictability of rheological models.
368 In developing a rheological model for nano-drilling muds, the Vipulanandan model was
369 modified using existing relationships. This includes relationships for the structural kinetics of
370 cohesive sediment suspensions and that which describes the interparticle behavior of
371 nanoparticles in aqueous solutions. A key advantage of this approach is that the shear stress is

372 expressed as a function of nanoparticles parameters in a very simplified form and eliminates
373 the need for a large number of tuning parameters. The significance of this outcome is that the
374 impact of nanoparticles (as captured by size, material property and concentration) on the
375 drilling mud rheology can be directly inferred during computational modelling using a single
376 fitting parameter. This parameter, known as a tuning parameter in this work, helps to account
377 for uncertainties surrounding nanoparticle interaction with clay particles. These uncertainties
378 are known to arise from the changing surface properties of the nanoparticles and bentonite
379 clay particles due to interactions. This approach helps to reduce the complexity of having a
380 lot of fitting parameters and over parameterization associated with known models developed
381 for nano-drilling muds. The modified Vipulanandan show better prediction for a 6.3 wt.%
382 mud with R^2 of 0.999 compared to 0.962 for Power law and 0.991 for Bingham. However,
383 the R^2 value was the same with Herschel Buckley model but the RMSE value show better
384 prediction for the Vipulanandan model with a value of 0.377 Pa compared to the 0.433 Pa for
385 Herschel Buckley model. Validation of this was carried out by applying statistical tools the
386 design matrix formed from the experimental analysis. The statistical evaluation further show
387 the significance of these interactions between nanoparticles and clay particles and its impact
388 on the rheological properties of the mud. Future works may consider incorporating the effects
389 of temperature and salinity in the modified Vipulanandan model. This can be achieved by
390 relating the associated time constants of the modified model with the characteristic equation
391 for the rotational diffusion of particles. This approach would further reduce the uncertainty
392 surrounding nanoparticle interaction with clay particles under extreme reservoir conditions.

393 **Nomenclature**

394 *Abbreviations*

395 DR	Dial Readings
396 RPM	Revolutions per Minutes

397	PV	Plastic Viscosity
398	YP	Yield Point
399	AV	Apparent Viscosity
400	<i>Symbols</i>	
401	τ_0	Yield Point, Pa
402	τ	Shear Stress, Pa
403	$\dot{\gamma}$	Shear Rate, s⁻¹
404	τ_p	Shear Stress due to Nanoparticles, Pa
405	τ_∞	Shear Stress measured at high Shear Rates, Pa
406	μ_∞	Viscosity at Infinite Shear Rate, Pas
407	ϕ	Volume Fraction of Nanoparticles
408	d_p	Diameter of Nanoparticles, nm
409	r_p	Radius of Nanoparticles, nm
410	A_p	Surface Area of Nanoparticles, nm²
411	A_o	Haymaker's Constant, J
412	β	Parameter Constant in the Model of Gerogiorgis et al. (2017), s
413	C_b	Bentonite Content, wt.%
414	C_n	Nanoparticle Concentration, vol.%
415	F_{vdw}	Van der Waals Force, N
416	H	Interparticle Distance between Nanoparticles, nm
417	τ_{Ci}	Shear Stress at a Reference Point (without nanoparticles), Pa
418	τ_{lim}	Shear Stress Limit, Pa
419	A	Parameter Constant in Vipulanandan Model, [Pas]⁻¹
420	D	Parameter Constant in Vipulanandan Model, Pa⁻¹
421	β_0	Tuning Parameter in the Modified Vipulanandan Model, Pa

422	β_1	Time Costant in the Modified Vipulanandan Model, s
423	β_2	Parameter Constant in the Modified Vipulanandan Model, Pas
424	β_3	Time Constant in the Modified Vipulanandan Model, s
425	K	Consistency Index, [(Pa) s ⁿ]
426	n	Flow Index
427	μ_p	Plastic Viscosity, Pas
428	a_s, b_s and c_s	Parameter Constants in Sisko Model,
429	γ_0	Parameter Constant in Robertson-Stiff & Modified Robertson-Stiff Model,
430	s ⁻¹	
431	A_t and B_p	Parameter Constants in Prandtl-Eyring Model.
432	λ	Dimensionless Structuring parameter

433 **Acknowledgement**

434 The authors would like to appreciate the management of Covenant University for providing
435 an enabling environment to carry out this research.

436 **Funding**

437 This research did not receive any specific grant from funding agencies in the public,
438 commercial, or not-for-profit sectors.

439 **Conflict of Interest**

440 The authors have no potential conflict of interest to declare regarding the publication of this
441 article.

442 **References**

- 443 Abdo, J., & Danish Haneef, M. (2012). Nano-Enhanced Drilling Fluids: Pioneering Approach
444 to Overcome Uncompromising Drilling Problems. *Journal of Energy Resources*
445 *Technology, 134*, 1-6.
- 446 Abu-Jdayil, B. (2011). Rheology of Sodium and Calcium Bentonite-Water Dispersions:
447 Effect of Electrolytes and Aging Time. *International Journal of Mineral Processing*,
448 *98*, 208-213.
- 449 Afolabi, R. O., & Yusuf, E. O. (2018). Nanotechnology and the Global Energy Demand:
450 Challenges and Prospects for a Paradigm Shift in the Oil and Gas Industry. *Journal of*
451 *Petroleum Exploration and Production Technology*, 1-19.
- 452 Afolabi, R. O., Orodu, O. D., & Efeovbokhan, V. E. (2017a). Properties and application of
453 Nigerian bentonite clay deposits for drilling mud formulation: Recent advances and
454 future prospects. *Applied Clay Science, 143*, 39-49.
- 455 Afolabi, R. O., Orodu, O. D., Efeovbokhan, V. E., & Rotimi, O. J. (2017b). Optimizing the
456 rheological properties of silica nano-modified bentonite mud using overlaid contour
457 plot and estimation of maximum or upper shear stress limit. *Cogent Engineering, 4*, 1-
458 18.
- 459 Fan, H., Zhou, H., Meng, X., Gao, J., & Wang, G. (2015). Accurate Prediction Model for
460 Rheological Properties of Drilling Fluids at High Temperature and High Pressure
461 Conditions. *SPE/IATMI Asia Pacific Oil & Gas Conference and Exhibition* (pp. 1-14).
462 Bali, Indonesia: Society of Petroleum Engineers.
- 463 Fazelabdolabadi, B., Khodadadi, A. A., & Sedaghatzadeh, M. (2015). Thermal and
464 Rheological Properties Improvement of Drilling Fluids using Functionalized
465 Nanotubes. *Applied Nanoscience, 5*, 651-659.

- 466 Gerogiorgis, D. I., Reilly, S., Vryzas, Z., & Kelessidis, V. C. (2017). Experimentally
467 Validated First-Principles Multivariate Modeling for Rheological Study and Design of
468 Complex Drilling Nanofluid Systems. *SPE/IADC Drilling Conference and Exhibition*
469 (pp. 1-11). Hague: Society of Petroleum Engineers.
- 470 Hoelscher, K. P., Stefano, G., Riley, M., & Young, S. (2012). Application of Nanotechnology
471 in Drilling Fluids. *SPE International Oilfield Nanotechnology Conference* (pp. 1-7).
472 Noordwijk: Society of Petroleum Engineers.
- 473 Ismail, A. R., Aftab, A., Ibupoto, Z. H., & Zolkifile, N. (2016). The Novel Approach for the
474 Enhancement of Rheological Properties of Water-Based Drilling Fluids by using
475 Multi-Walled Carbon Nanotube, Nanosilica and Glass Beads. *Journal of Petroleum*
476 *Science and Engineering*, 139, 264-275.
- 477 Jung, C. M., Zhang, R., Chenevert, M., & Sharma, M. (2013). High Performance Water-
478 Based Mud using Nanoparticles for Shale Reservoirs. *Unconventional Resources*
479 *Technology Conference* (pp. 1-7). Denver: Society of Petroleum Engineers.
- 480 Kelessidis, V. C., & Maglione, R. (2008). Yield Stress of Water-Bentonite Dispersions.
481 *Colloids and Surfaces A: Physicochemical and Engineering Aspects*, 318, 217-226.
- 482 Lee, E. J., Stefanus, C., & Leong, Y. K. (2012). Structural Recovery Behaviour of Kaolin,
483 Bentonite and K-Montmorillonite Slurries. *Powder Technology*, 223, 105-109.
- 484 Liberman, A., Mendez, N., Trogler, W. C. & Kummel, A. C. (2014). Synthesis and surface
485 functionalization of silica nanoparticles for nanomedicine. *Surface Science Reports*,
486 69(2 - 3), 132-158.
- 487 Mahmoud, O., Nasr El-Din, H., Vryzas, Z., & Kelessidis, V. (2016). Nanoparticle Based
488 Drilling Fluids for Minimizing Formation Damage in HP/HT Applications. *SPE*

- 489 *International Conference and Exhibition on Formation Damage and Control* (pp. 1-
490 26). Louisiana: Society of Petroleum Engineers.
- 491 Reilly, S., Vryzas, Z., Kelessidis, V. C., & Gerogiorgis, D. I. (2016). First Principles
492 Rheological Modelling and Parameter Estimation for Nanoparticle Based Smart
493 Drilling Fluids. *European Symposium on Computer Aided Process Engineering* (pp.
494 1-6). Portoroz: Elsevier B. V.
- 495 Toorman, E. A. (1997). Modelling the Thixotropic Behaviour of Dense Cohesive Sediment
496 Suspensions. *Rheologica Acta*, 36(1), 56-65.
- 497 Vipulanandan, C., & Mohammed, A. S. (2014). Hyperbolic Rheological Model with Shear
498 Stress Limit for Acrylamide Polymer Modified Bentonite Drilling Muds. *Journal of*
499 *Petroleum Science and Engineering*, 122, 38-47.
- 500 Vryzas, Z., & Kelessidis, V. C. (2017). Nano-Based Drilling Fluids: A Review. *Energies*, 10,
501 1-34.
- 502 Yoon, J., & El-Mohtar. (2013). Dynamic Rheological Properties of Sodium Pyrophosphate
503 Modified Bentonite Suspensions for Liquefaction Mitigation. *Clays Clay Minerals*,
504 61, 319-327.
- 505 Zakaria, M. F., Husein, M., & Hareland, G. (2012). Novel nanoparticle-Based Drilling Fluid
506 with Improved Characteristics. *SPE International Oilfield Nanotechnology*
507 *Conference* (pp. 1-6). Noordwijk: Society of Petroleum Engineers.

508

509

Table 1: Rheological models and their predictive capabilities based on the conditions described in equations (1) to (4).

Rheological Model	Equation ($\tau = f(\dot{\gamma})$)	$\lim_{\dot{\gamma} \rightarrow 0} \tau = \tau_0$	$\frac{d\tau}{d\dot{\gamma}} > 0$	$\frac{d^2\tau}{d\dot{\gamma}^2} < 0$	$\lim_{\dot{\gamma} \rightarrow \infty} \tau = \tau_{\max}$
Bingham Plastic	$\tau = \tau_0 + \mu_p \dot{\gamma}$	τ_0	μ_p	0	∞
Power Law	$\tau = K\dot{\gamma}^n$	0	$Kn\dot{\gamma}^{n-1}$	$Kn(n-1)\dot{\gamma}^{n-2}$	∞
Herschel Buckley	$\tau = \tau_0 + K\dot{\gamma}^n$	τ_0	$Kn\dot{\gamma}^{n-1}$	$Kn(n-1)\dot{\gamma}^{n-2}$	∞
Casson	$\tau = (\tau_0^{1/2} + \mu_p^{1/2}\dot{\gamma}^{1/2})^2$	τ_0	$\frac{\mu_p\dot{\gamma}^{1/2} + \tau_0^{1/2}\mu_p^{1/2}}{(\dot{\gamma}^{1/2})}$	$\frac{\mu_p}{2\dot{\gamma}} - \left(\frac{\mu_p\dot{\gamma}^{1/2} + \tau_0^{1/2}\mu_p^{1/2}}{2(\dot{\gamma}^{3/2})}\right)$	∞
Sisko	$\tau = a_s\dot{\gamma} + b_s\dot{\gamma}^{c_s}$	0	$a_s + b_s c_s \dot{\gamma}^{c_s-1}$	$b_s c_s^2 \dot{\gamma}^{c_s-2}$	∞
Robertson-Stiff	$\tau = K(\gamma_0 + \dot{\gamma})^n$	$K(\gamma_0)^n$	$Kn(\gamma_0 + \dot{\gamma})^{n-1}$	$Kn(n-1)(\gamma_0 + \dot{\gamma})^{n-2}$	∞
Modified Robertson Stiff	$\tau = \tau_0 + K(\gamma_0 + \dot{\gamma})^n$	$\tau_0 + K(\gamma_0)^n$	$Kn(\gamma_0 + \dot{\gamma})^{n-1}$	$Kn(n-1)(\gamma_0 + \dot{\gamma})^{n-2}$	∞
Prandtl-Eyring	$\tau = A_t \sinh^{-1}\left(\frac{\dot{\gamma}}{B_p}\right)$	0	$\frac{A_t}{B_p \sqrt{\frac{\dot{\gamma}^2}{B_p^2} + 1}}$	$-\frac{A_t \dot{\gamma}}{B_p^3 \left(\frac{\dot{\gamma}^2}{B_p^2} + 1\right)^{3/2}}$	∞
Vipulanandan	$\tau = \tau_0 + \frac{\dot{\gamma}}{A + D\dot{\gamma}}$	τ_0	$\frac{A}{(A + D\dot{\gamma})^2}$	$\frac{-2AD}{(A + D\dot{\gamma})^3}$	$\tau_0 + \frac{1}{D}$

Table 2: Parameter constants of the modified Vipulanandan model for drilling mud with varying bentonite content containing 0.2 vol.% silica nanoparticles at 25^oC.

Bentonite Content, C_b (wt.%)	Tuning Parameter, β_o (Pa)	Time Constant, β_1 (s)	Viscosity Parameter, β_2 (Pas)	Time Constant, β_3 (s)
0	0	0	0	0
6.3	0.00014	0.00039	0.0063	0.0807
13	0.00850	0.00090	0.0367	0.0096
15	0.36640	0.00110	0.0820	0.0040

Table 3: Parameter constants of the modified Vipulanandan model for 13 wt.% drilling mud containing 0.2 to 0.6 vol.% silica nanoparticles at 25°C.

Nanoparticle Concentration (vol.%)	Tuning Parameter, β_0 (Pa)	Time Constant, β_1 (s)	Viscosity Parameter, β_2 (Pas)	Time Constant, β_3 (s)
0	0	0.0008	0.0361	0
0.2	0.0085	0.0009	0.0367	0.0096
0.4	0.2261	0.0006	0.0295	0.0318
0.6	0.4209	0.0011	0.0410	0.0319

Table 4: Experimental design matrix obtained analysed using the central composite design (CCD) and the predicted rheological properties of the nano-drilling mud.

Bentonite Content (wt.%)	Silica Nanoparticles (vol.%)	Plastic Viscosity (Pas)	Yield Point (Pa)	Apparent Viscosity (Pas)
6.3	0.0	0.0034	2.1449	0.0055
6.3	0.2	0.0035	2.5535	0.0060
6.3	0.4	0.0036	2.5535	0.0061
6.3	0.6	0.0037	2.6046	0.0063
13	0.0	0.0120	22.982	0.0350
13	0.2	0.0130	25.535	0.0375
13	0.4	0.0130	28.089	0.0405
13	0.6	0.0130	31.663	0.0440
15	0.0	0.0170	62.816	0.0785
15	0.2	0.0230	68.945	0.0905
15	0.4	0.0280	66.391	0.0940
15	0.6	0.0300	67.923	0.0955

Table 5: Comparison between experimental and predicted shear stress limit for bentonite mud

Bentonite (wt.%)	Shear Stress Limit (Experimental Approach)	Shear Stress Limit (Vipulanandan Model – Eqn 24)
6.0	15.32	14.25
9.0	33.71	32.07
11.0	63.84	62.24

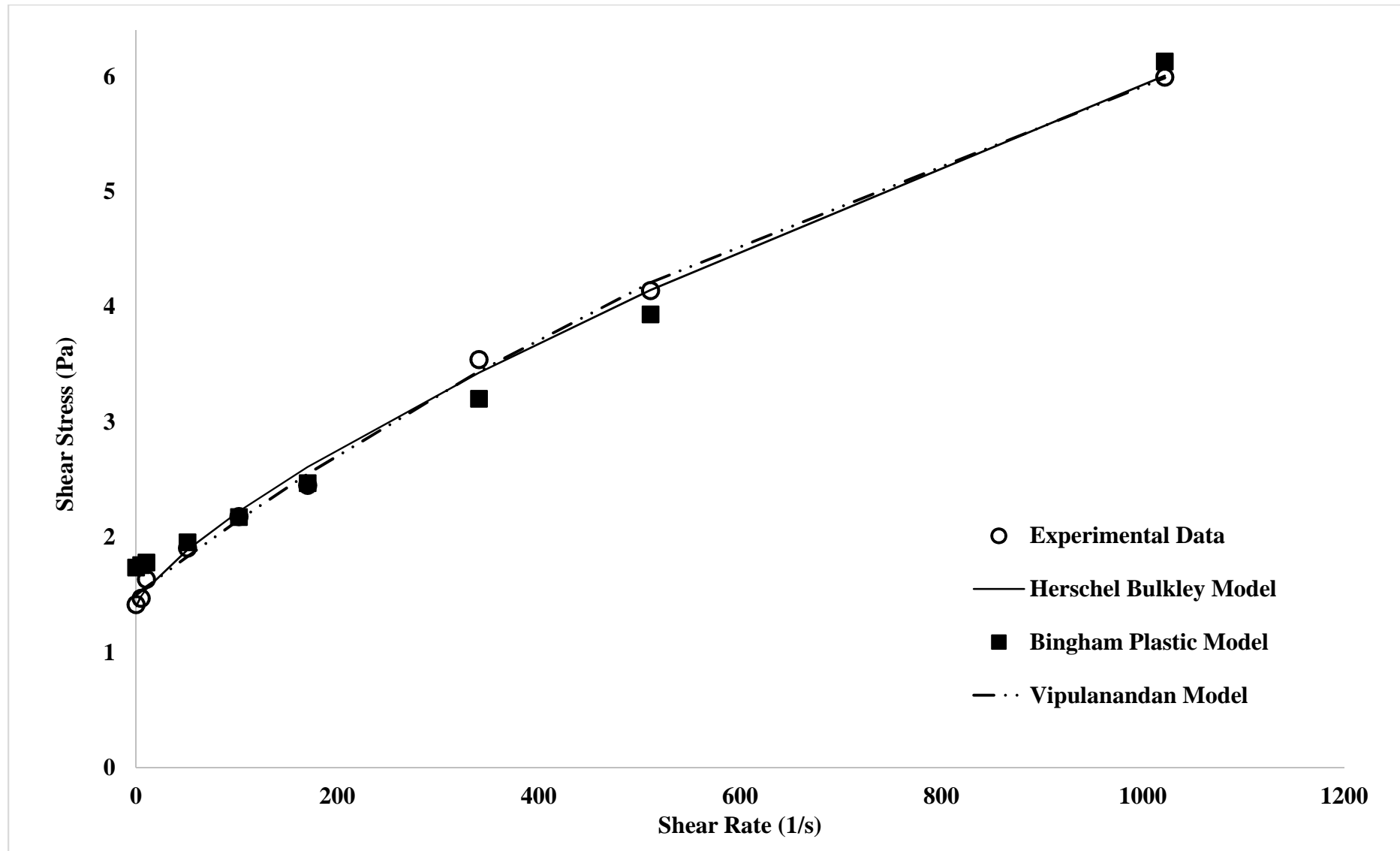


Figure 1: Rheological models applied to viscometric data obtained for 6.3wt.% bentonite mud at 25°C

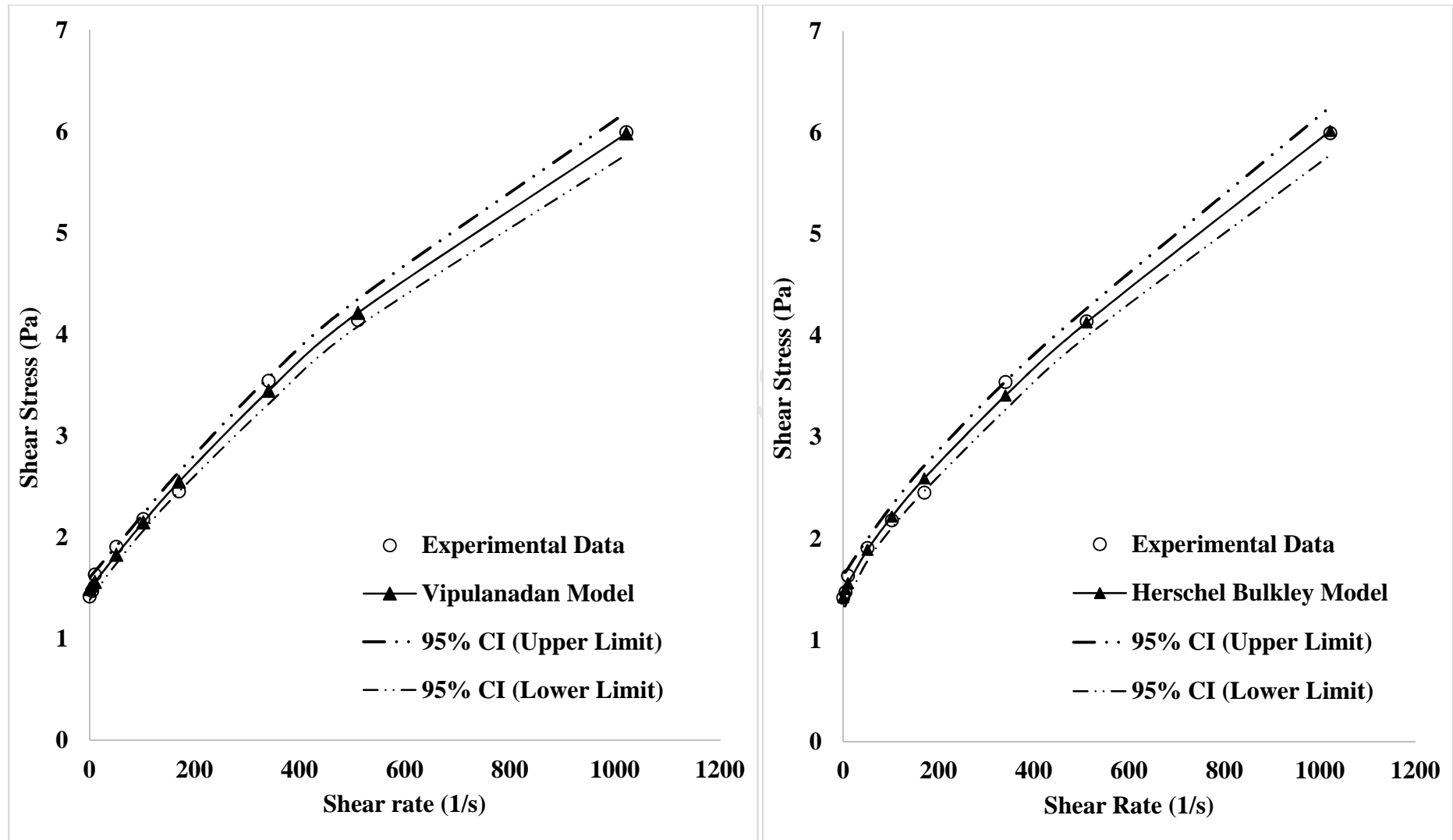


Figure 2: The prediction for Vipulanandan and Herschel Bulkley models at 95% confidence interval (CI) using viscometric data obtained for 6 wt.% bentonite mud at a temperature of 25°C

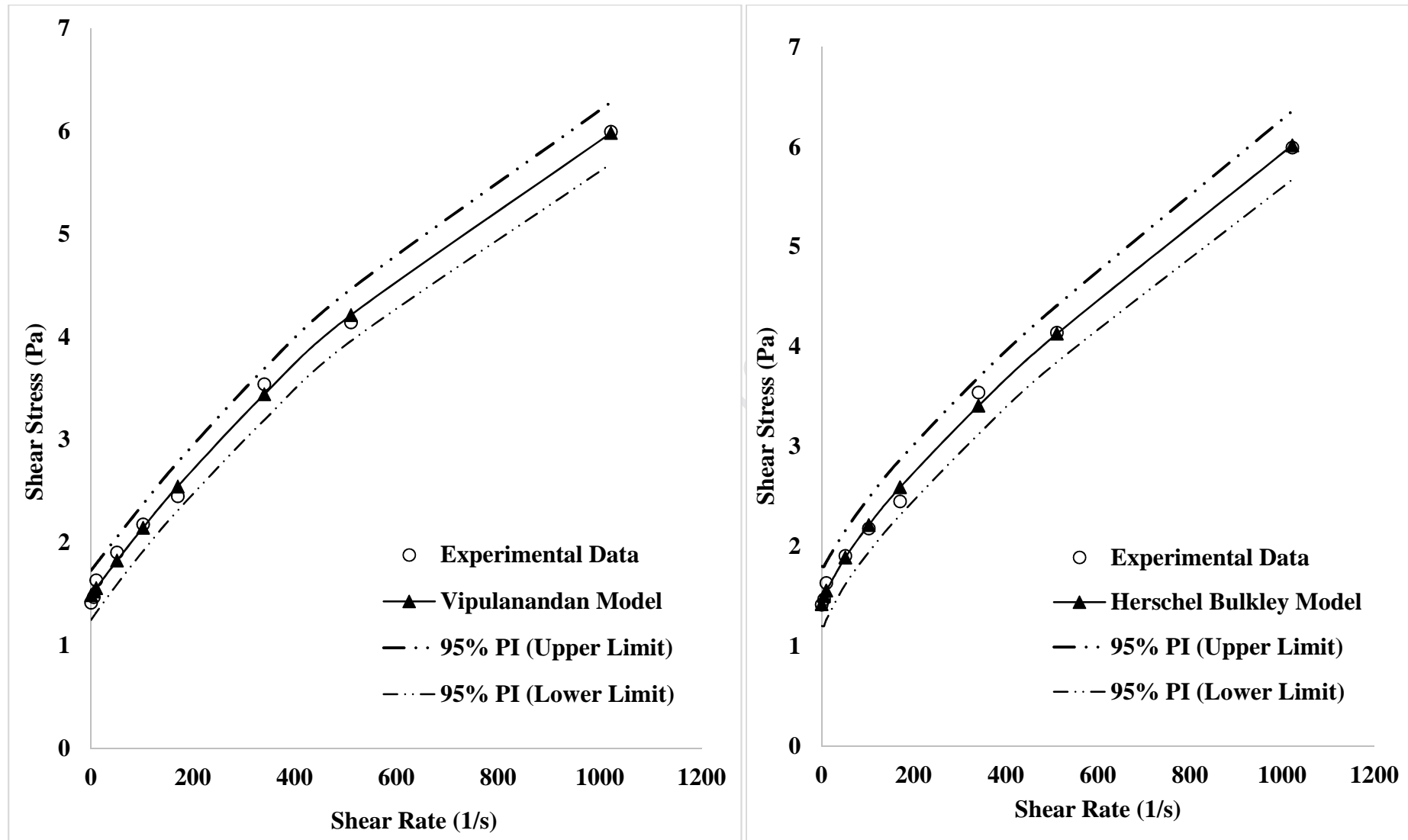


Figure 3: The prediction for Vipulanandan and Herschel Bulkley models at 95% prediction interval (PI) using viscometric data obtained for 6.3 wt.% bentonite mud at a temperature of 25°C

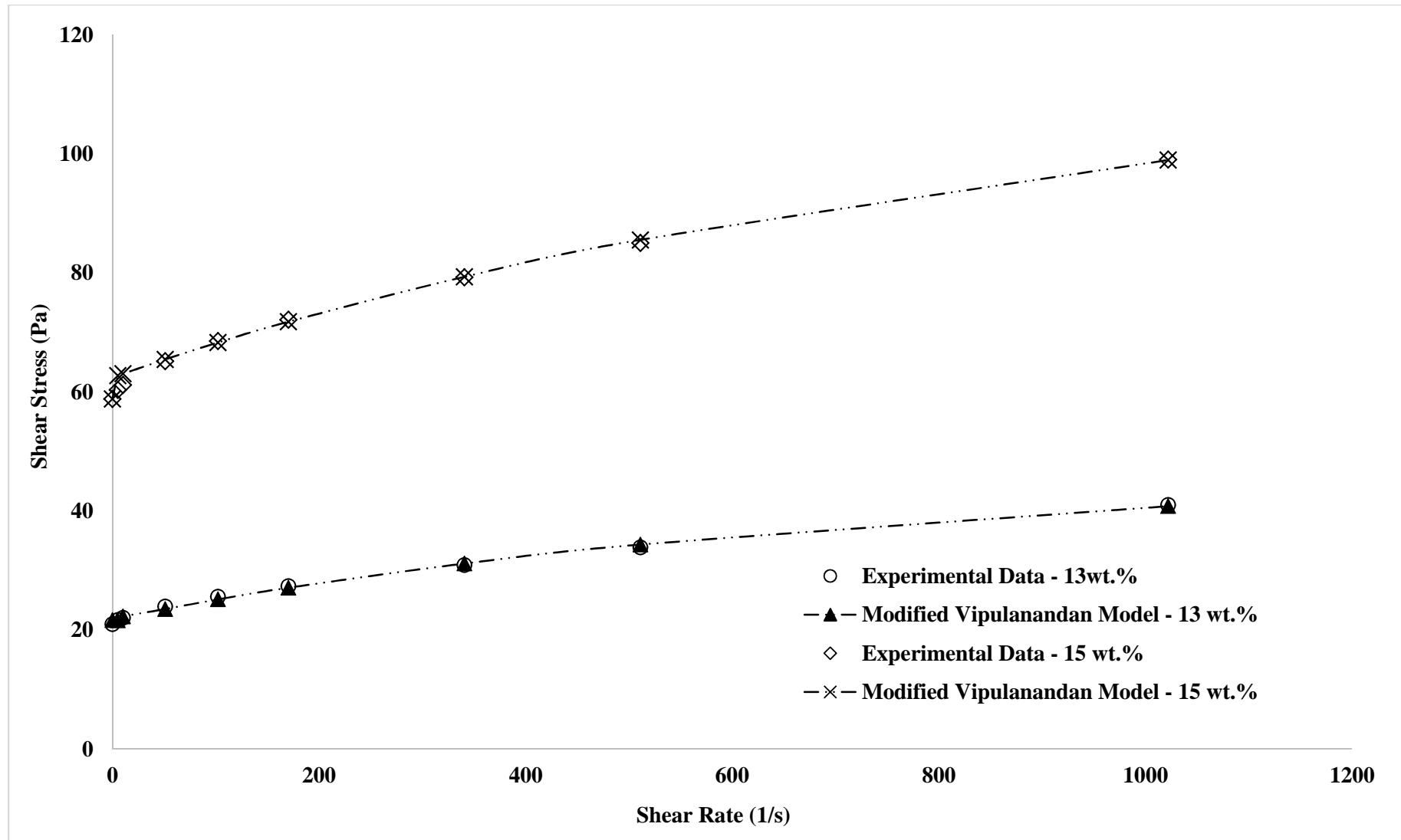


Figure 4: Fitted modified Vipulanandan model to rheological data for drilling mud containing 13, 15 wt.% bentonite clay and 0.2 vol.% silica nanoparticles at 25°C

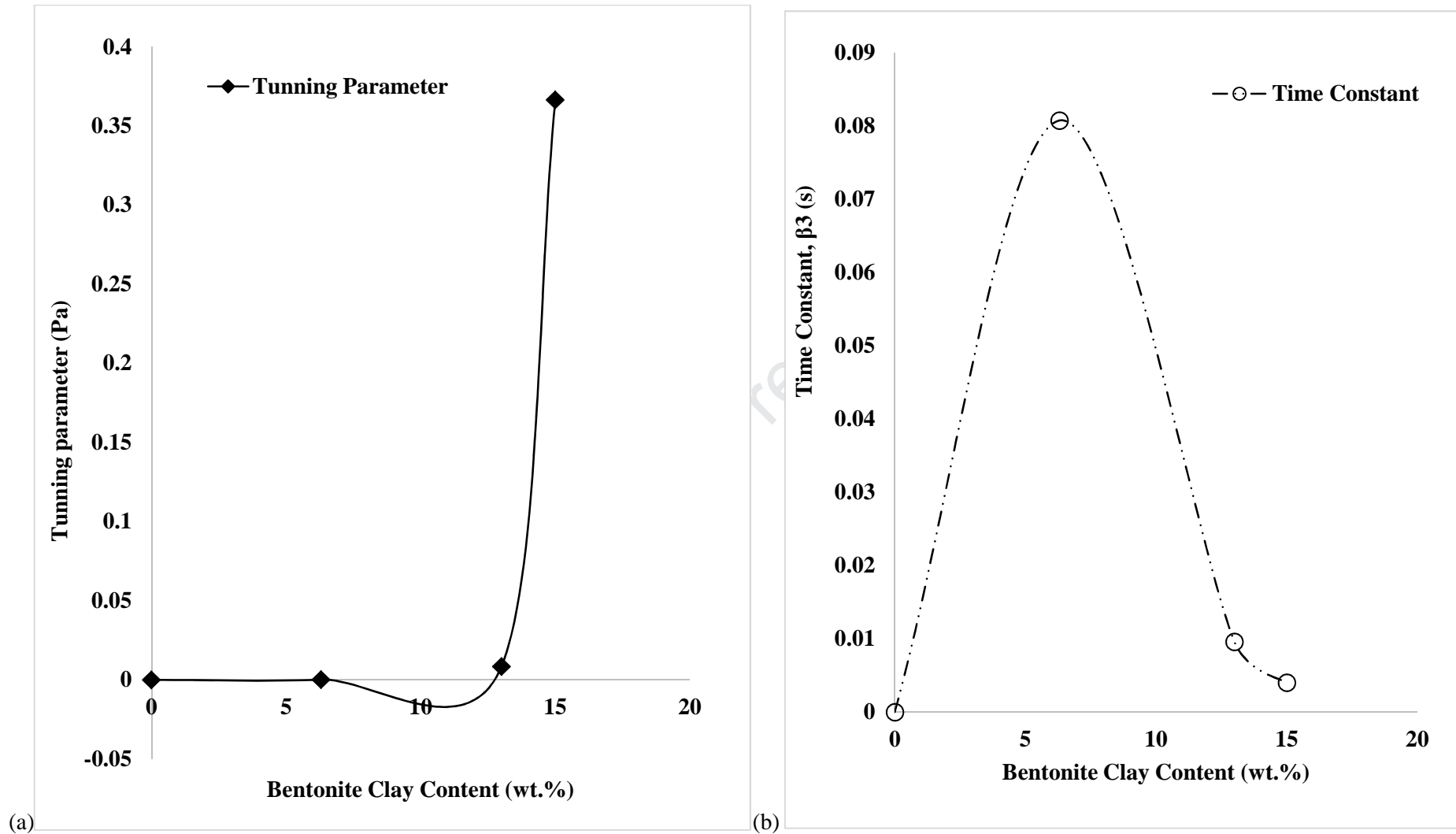


Figure 5: Effect of bentonite content on (a) the tuning parameter, β_0 and (b) the time constant, β_3 for a drilling mud containing 0.2 vol.% silica nanoparticles at 25°C.

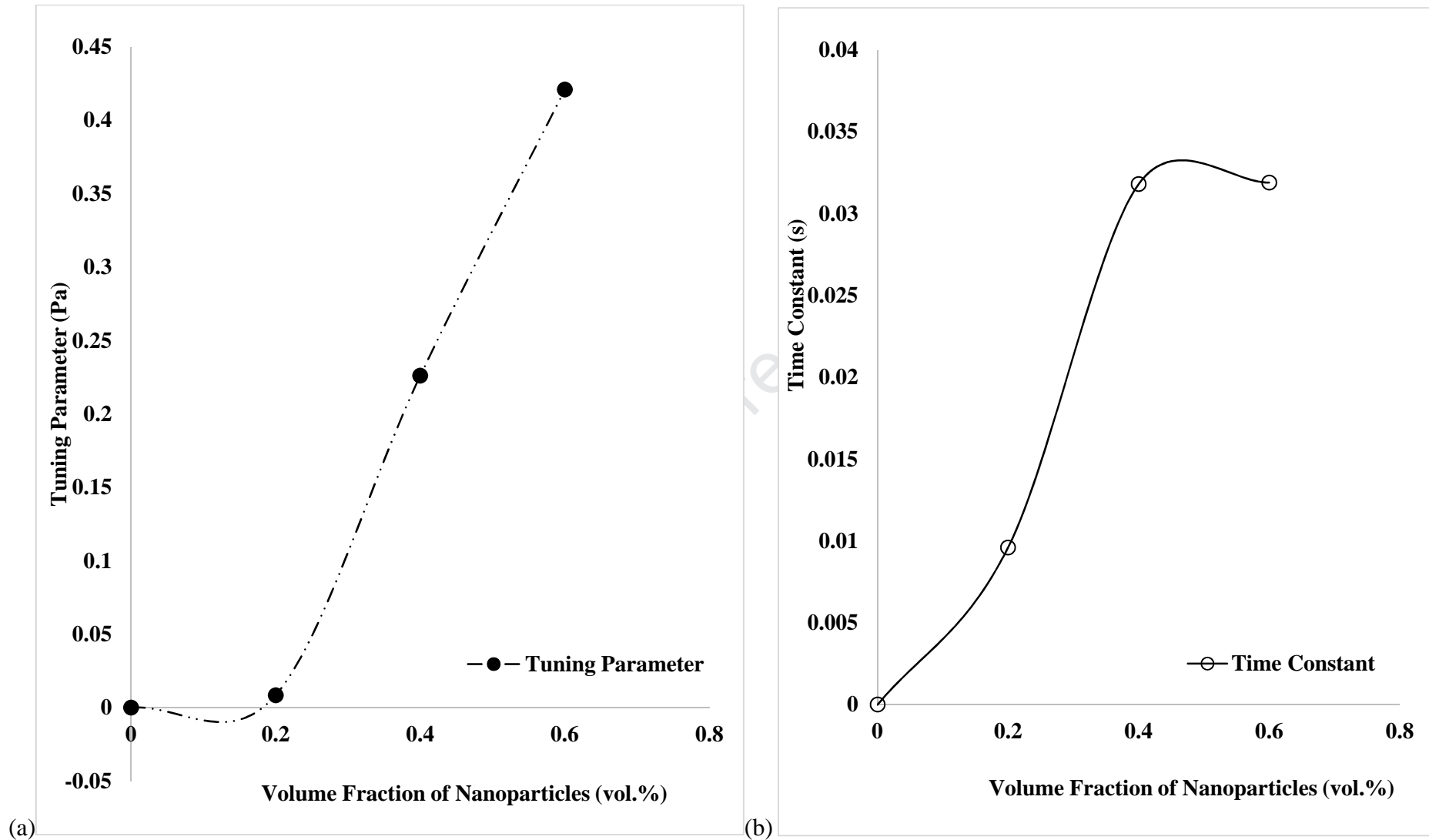


Figure 6: Effect of volume fraction of nanoparticles on (a) the tuning parameter, β_0 and (b) the time constant, β_3 for a drilling mud containing 13 wt.% bentonite clay at 25°C.

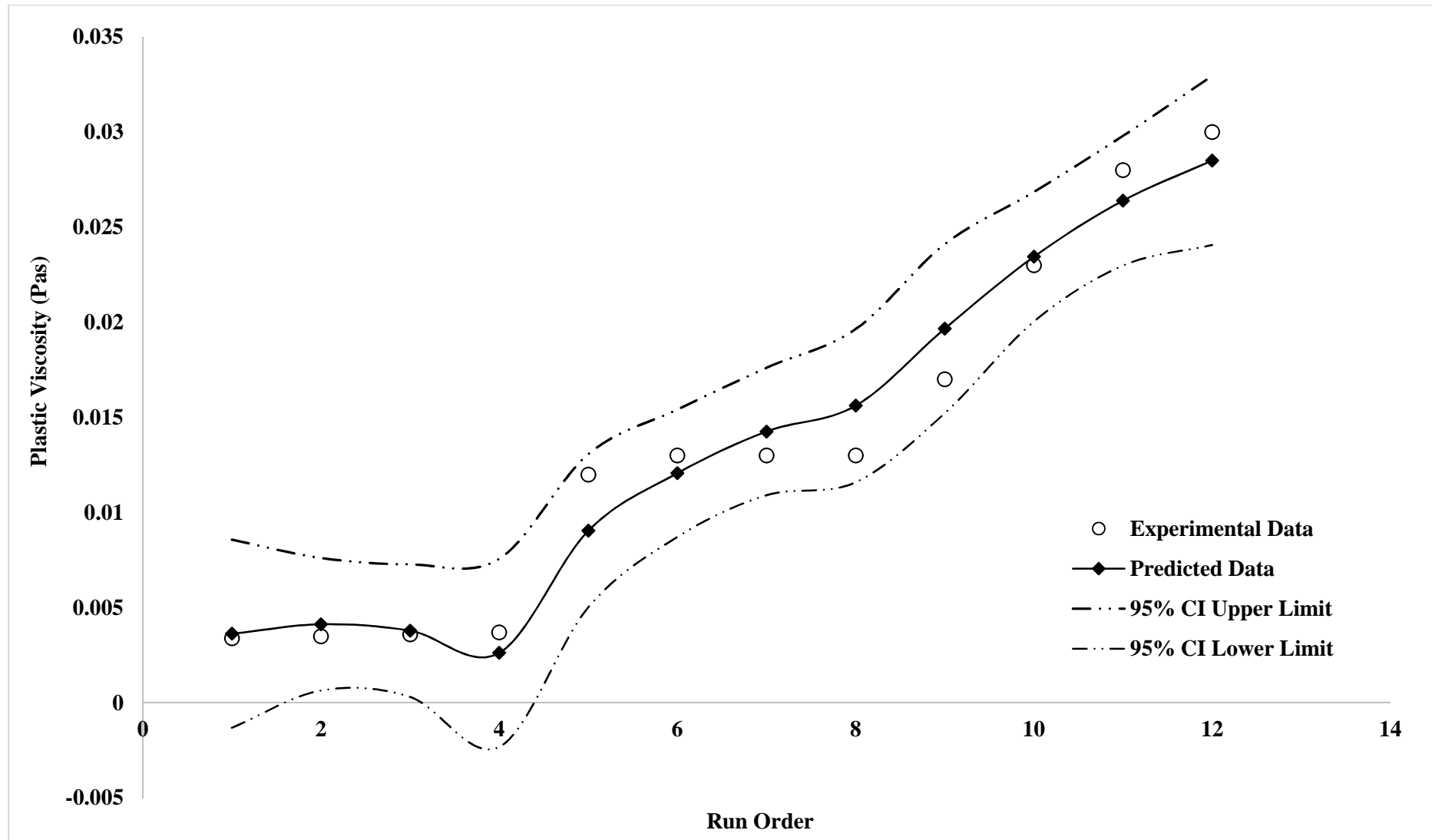


Figure 7: The 95% confidence interval for the statistical model obtained for plastic viscosity in (21) using the experimental design matrix of Table 4.

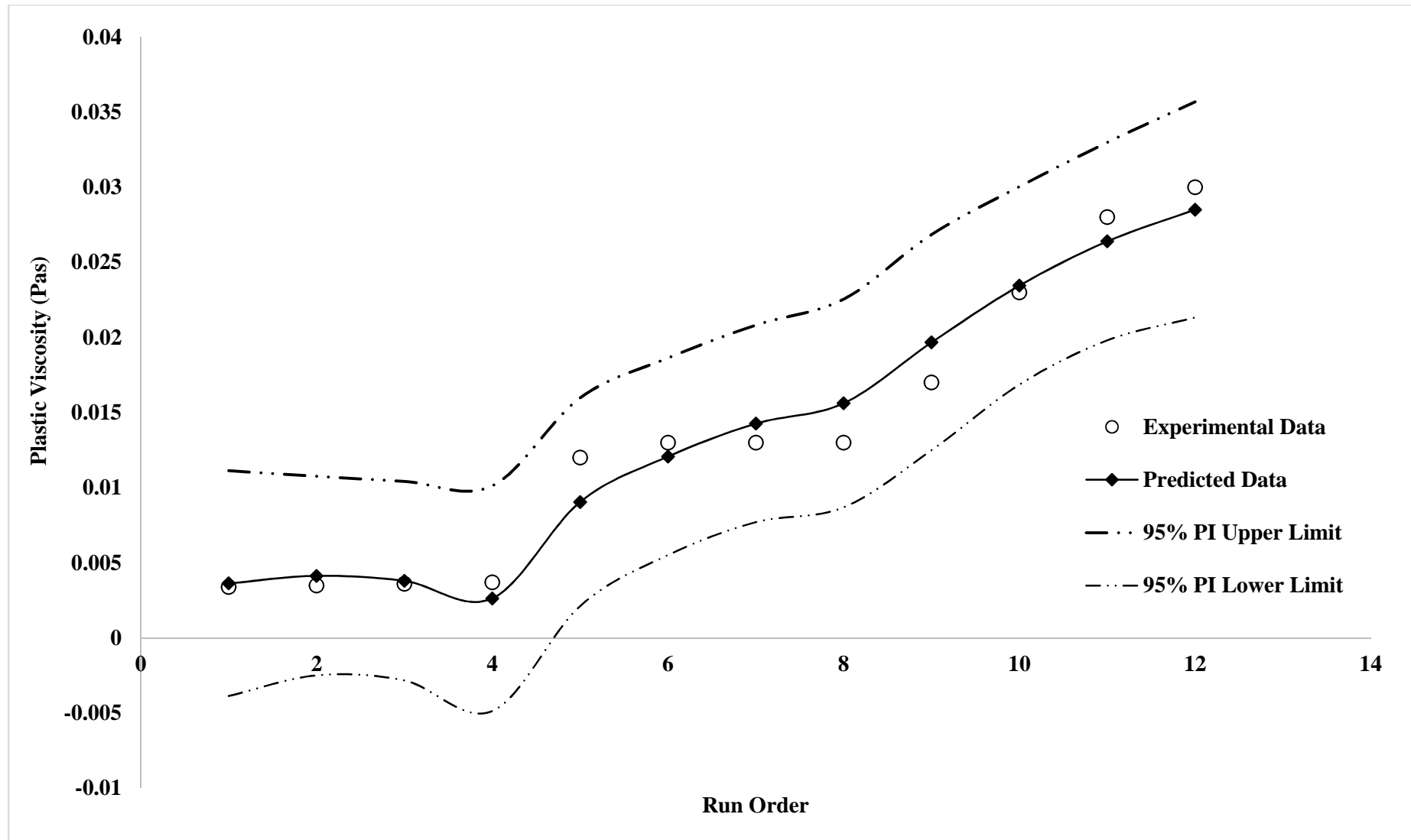


Figure 8: The 95% prediction interval (PI) for the statistical model obtained for plastic viscosity in (21) using the experimental design matrix of Table 4.

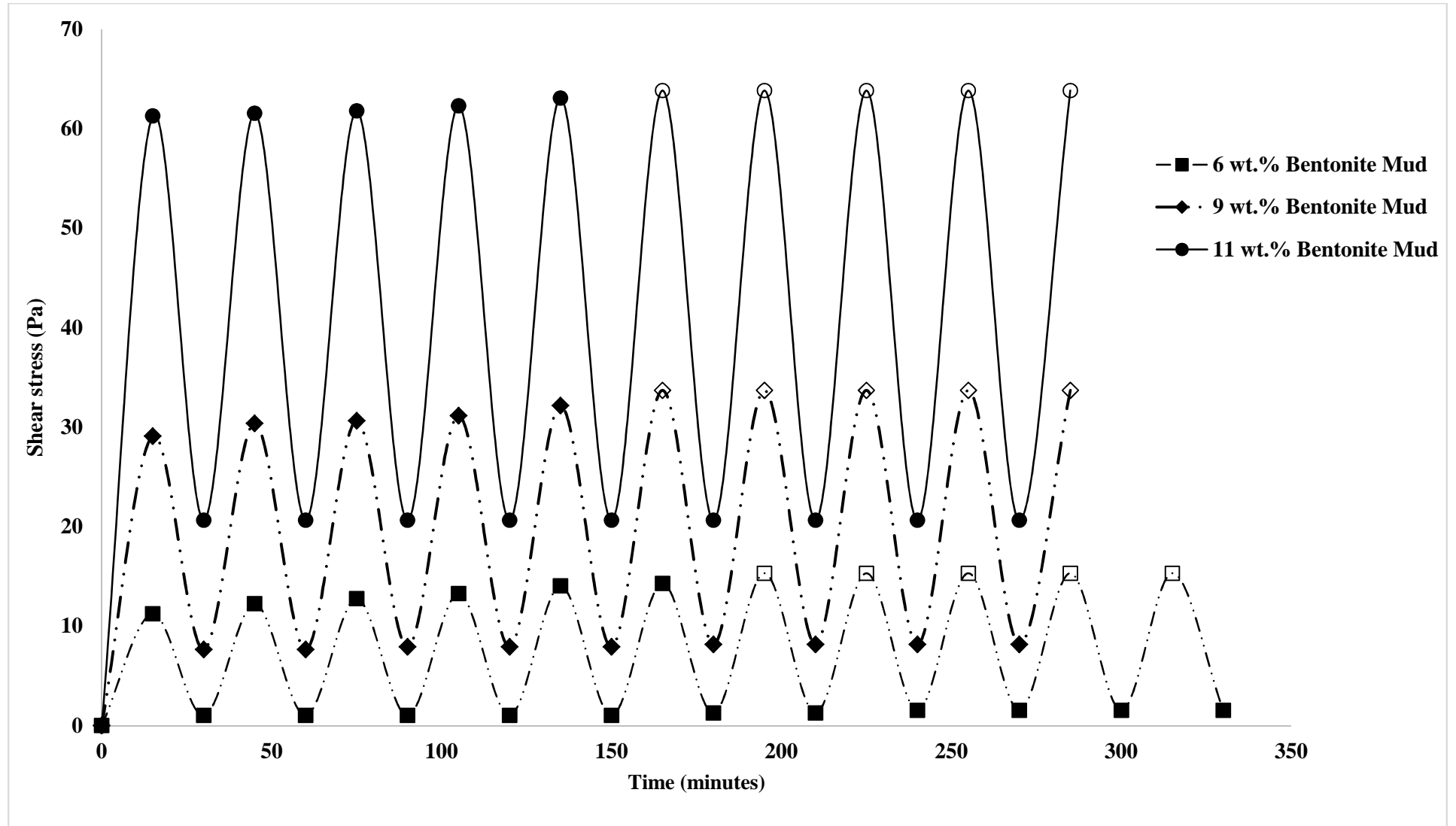


Figure 9: Experimental validation results for shear stress limit prediction for 6, 9 and 11 wt.% bentonite mud at shear rate of 1022 s^{-1} and temperature of $25 \text{ }^{\circ}\text{C}$. The open marker (no fill) corresponds to the constant shear stress values, which approximates the shear stress limit predicted by equation (24).

Highlights

- The Vipulanandan rheological model was modified to account for nanoparticle effect.
- This novel approach ensured few fitting parameter compared to other nano-models.
- This ensured that the complexity of the computational modelling was simplified.
- A tuning parameter was used to account for the uncertainty arising from nanoparticle – clay particle interaction.

Journal Pre-proof